Physics – Uspekhi **57** (1) 66 – 79 (2014)

INSTRUMENTS AND METHODS OF INVESTIGATION PACS numbers: 13.25.Gv, 13.66.Bc, 13.66.Jn, 14.40.Lb, 14.60.Fg

High-precision particle mass measurements using the KEDR detector at the VEPP-4M collider

E B Levichev, A N Skrinsky, Yu A Tikhonov, K Yu Todyshev

DOI: 10.3367/UFNe.0184.201401c.0075

Contents

Abstract. A review is presented of experiments performed using the KEDR detector at the VEPP-4M accelerator complex for the precise measurement of particle masses. The resonant depolarization method, proposed in 1975 at the G I Budker Institute of Nuclear Physics of the RAS Siberian Branch for measuring beam energy, has undergone further development in the experiments described; an unprecedented accuracy of 5×10^{-7} has been achieved. Application of this method together with measurement of the Compton backscattering energy allowed a series of experiments to be carried out which have provided the world's most accurate mass values for the J/ψ, $\psi(2S)$, $\psi(3770)$, and $D^{\pm}$ mesons and for the τ-lepton.

E B Levichev Budker Institute of Nuclear Physics,
Siberian Branch of the Russian Academy of Sciences,
prosp. Akademika Lavrent'eva 11, 630090 Novosibirsk,
Russian Federation;
Novosibirsk State Technical University,
prosp. Marksa 20, 630092 Novosibirsk, Russian Federation
A N Skrinsky Budker Institute of Nuclear Physics,
Siberian Branch of the Russian Academy of Sciences,
prosp. Akademika Lavrent'eva 11, 630090 Novosibirsk,
Russian Federation
Yu A Tikhonov, K Yu Todyshev Budker Institute of Nuclear Physics,
Siberian Branch of the Russian Academy of Sciences,
prosp. Akademika Lavrent'eva 11, 630090 Novosibirsk,
Russian Federation;
Novosibirsk State University,
ul. Pirogova 2, 630090 Novosibirsk, Russian Federation
E-mail: todyshev@inp.nsk.su

Received 10 July 2013
Uspekhi Fizicheskikh Nauk **184** (1) 75 – 88 (2014)
DOI: 10.3367/UFNr.0184.201401c.0075
Translated by G Pontecorvo; edited by A Radzig

1. Introduction

Experiments devoted to precisely measuring the parameters of elementary particles have been and still remain an important component of modern high-energy physics. Thus, the urgent necessity can be understood of precise experiments in quarkonium spectroscopy, the results of which yield information on the quark–antiquark system, which serves as a stimulus for further development both of the theory of strong interactions and of field theory as a whole. And, while in the case of the quarkonium the measurement of masses paves the way to a hitherto unexplored region and serves as a benchmark for the theory, precise knowledge of the τ-lepton mass is necessary for a straightforward test of one of the principles underlying the Standard Model, namely, of the $\mu - \tau$-universality of electroweak interaction theory.

During the past decade, a series of experiments has been carried out at the Budker Institute of Nuclear Physics of the RAS Siberian Branch (RAS SB INP) on the precise measure-

ment of the masses of elementary particles, and, here, the masses of the narrow J/ψ and ψ(2S) resonances have been determined with an unperecedented high precision. A key role in these experiments is played by the resonant depolarization (RD) method elaborated and developed at RAS SB INP [1, 2]. Experiments carried out with the KEDR detector at the VEPP-4M accelerator complex[1] are a continuation of the series of measurements of the masses of bound heavy quark states, initiated 30 years ago with the experiments using the Olya [3] and MD-1 detectors (MD stands for magnetic detector) [4].

The greatest success in the studies of e^+e^--annihilation processes has been mostly achieved owing to the statistics collected at B-factories which provide high luminosity. At the same time, there are questions that can be answered only by applying the unique experimental techniques advanced in experiments at VEPP-4M. Joint application of the RD method for absolute calibration of the accelerator energy with a precision on record and of the inverse Compton scattering (ICS) method for continuous control of the electron beam energy makes it possible to carry out precise measurements of elementary particle masses at VEPP-4M.

In this article, results are presented of experiments devoted to measurement of the masses of the J/ψ-, ψ(2S)-, ψ(3770)-, and D-mesons and of the τ-lepton, which were obtained by the KEDR Collaboration between the years 2002 and 2012.

2. VEPP-4 accelerator-storage facility

Colliding beams serve as one of the main instruments in studies of elementary particles in modern high-energy physics. The VEPP-4 accelerator-storage facility [5, 6], with colliding electron–positron beams of energies from 2 up to 11 GeV in the center-of-mass system, permits resolving a broad range of problems in high-energy physics and carrying out studies of nuclear processes with internal targets, as well as experiments with synchrotron radiation (SR) and an extracted beam of tagged bremsstrahlung gamma-quanta. The possibilities provided by the facility are restricted by its insufficiently high luminosity, which in the case of VEPP-4M is significantly inferior to the luminosities of many other colliders. For this reason, the experimental program for the KEDR detector basically involves precise experiments for measuring the masses of elementary particles. Moreover, owing to the unique system for registering scattered electrons, studies of two-photon processes are possible.

VEPP-4 was commissioned in 1979. During the period between 1981 and 1985, the MD-1 detector [4] was utilized at VEPP-4 for carrying out numerous studies into the physics of ypsilon-mesons, on measuring R — the ratio of the total cross section of e^+e^--annihilation into hadrons and the Born cross section of e^+e^--annihilation into a muon pair — and in two-photon physics [7–17]. In 1986–1994, the ring underwent modernization for the installation of the KEDR detector and for enhancement of the accelerator luminosity. Renewal of the facility has permitted reducing the minimal operational accelerator energy to 1 GeV and made it possible to perform experiments on measuring R within a larger range of energies.

The VEPP-4M facility (Fig. 1) is composed of the VEPP-4M collider, the VEPP-3 booster-storage ring, and an injector system consisting of a linear electron accelerator, a conversion system, the B-4 synchrotron, and beam transportation channels [18–21]. The main parameters of VEPP-4M are presented in Table 1.

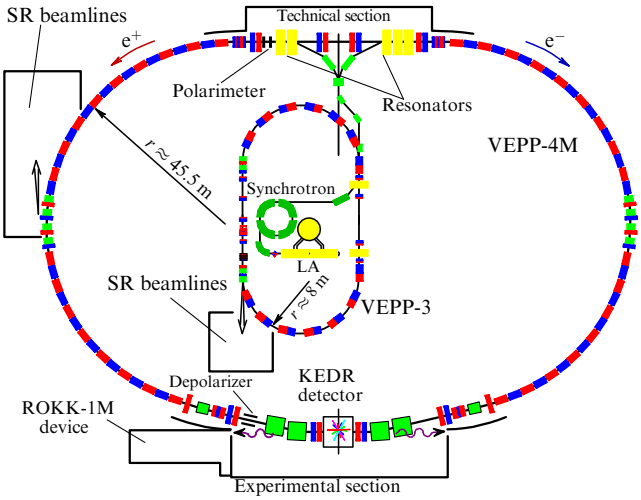

Figure 1. Layout of VEPP-4 accelerator-storage facility: ROKK is the abbreviation for 'backscattered Compton quanta' (in Russian), and LA is the linear accelerator.

Table 1. Parameters of VEPP-4M.

Parameter	Value
Circumference	366 m
Revolution radius	34.5 m
Maximum energy	5.5 GeV
Orbit compression factor	0.017
Number of bunches	2 × 2
Betatron tunes, horizontal/vertical	8.54/7.58
Frequency of high-frequency (HF) system	181.8 MHz
HF harmonic	222
Maximum HF voltage	5 MV
Structure functions at interaction point	
Vertical beta-function	0.05 m
Horizontal beta-function	0.75 m
Horizontal dispersion at interaction point	0.80 m

VEPP-4M has a perimeter 366 m long, and it consists of two semirings and two rectilinear sections, one of which accomodates accelerating resonators and the injection system, while the other one contains the KEDR detector together with other experimental equipment. For operation in the mode of 2 × 2 colliding bunches, plates for electrostatic beam separation are installed in the semirings. Two pairs of dipole magnets, placed inside the experimental section, together with quadrupole lenses of the final focus represent a strong-focusing spectrometer in the system for scattered electrons within the KEDR detector. Two dipole and two gradient wigglers permit controling the size of the beam and the damping decrements

For VEPP-4M operation in the 2 × 2 bunch mode at a beam energy of 2 GeV, the peak luminosity amounts to 3×10^{30} cm^{-2} s^{-1}. When the beam energy exceeds 4 GeV, the luminosity amounts to about 2×10^{31} cm^{-2} s^{-1} with the existing injection system. Putting the new injection system [22] into operation at a beam energy of 5 GeV will permit achieving a peak luminosity of up to 8×10^{31} cm^{-2} s^{-1}. As

[1] VEPP is the Russian abbreviation for 'vstrechnye electron-positronnye puchki' ('colliding electron–positron beams').

has been shown experimentally, the transverse and longitudinal feedback systems installed at VEPP-4M in this case permit obtaining a current of up to 40 mA in a single bunch. The existing injector complex intended for the injection of e^+ and e^- beams into the VEPP-3 storage ring operates at a repetition rate of 1.5 Hz and includes a two-section linear accelerator (LA) (energy up to 50 MeV) and the B-4 synchrotron (energy up to 350 MeV). In the injection mode of electrons, they are accelerated in the first LA section, then decelerated to an energy of 7 MeV in the second section, and then transported to the B-4 synchrotron for further acceleration and release. In the positron injection mode, the electrons accelerated in the LA up to a maximum energy of 50 MeV impinge upon the tungsten target-converter that produces electron–positron pairs. The positrons with an energy of 7 MeV are directed, with the aid of a focusing solenoid lens, toward B-4, where they are accelerated up to an energy of 350 MeV. Upon extraction from the synchrotron, the beam is injected into the VEPP-3 booster storage ring with the following parameters: maximum energy 2 GeV, electron current up to 150 mA, positron current up to 50 mA, and perimeter of 75 m. The characteristic accumulation rate of electrons in VEPP-3 amounts to 2–3 mA s^{-1}, and the positron accumulation rate ranges 30–50 μA s^{-1}. Since the electron and positron beams travel in the same direction in VEPP-3, alternation of the electron and positron accumulation modes is achieved by changing the polarity of the magnetic system.

3. KEDR detector

The KEDR universal detector [23–25] with a longitudinal magnetic field was developed at RAS SB INP for experiments at the VEPP-4M e^+e^- collider. The layout of the detector is presented in Fig. 2.

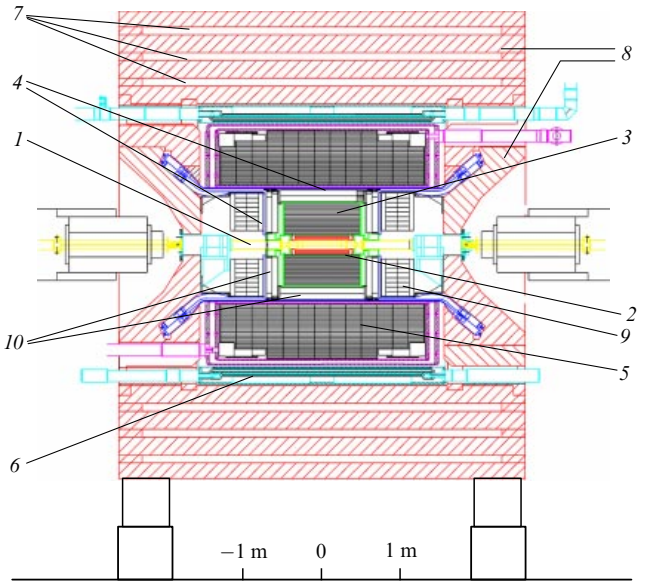

Figure 2. Layout of KEDR detector (longitudinal section): 1 — vacuum chamber, 2 — vertex detector, 3 — drift chamber, 4 — time-of-flight system, 5 — cylindrical liquid krypton (LKr)-based calorimeter, 6 — electromagnet coil, 7 — muon system, 8 — magnet yoke, 9 — endcap CsI crystals-based calorimeter, and 10 — aerogel Cherenkov counters.

The detector is composed of a coordinate system, a time-of-flight system based on scintillation counters, an electromagnetic calorimeter, a set of aerogel threshold counters, and a muon system based on streamer tubes. A longitudinal magnetic field of up to 0.6 T, necessary for determining the signs of charges and the momenta of charged particles, is produced by a superconducting solenoid. The coordinate system includes a vertex detector and a drift chamber. The momentum resolution of the tracking system in a field of 0.6 T amounts to $\sigma_{p_\perp}/p_\perp = [0.03^2 + (0.02p_\perp)^2]^{1/2}$, where the transverse momentum $p_\perp$ is expressed in GeV/c units. The electromagnetic calorimeter consists of a cylindrical LKr calorimeter (of thickness 14.8 X_0, where X_0 is the radiation unit of length) of mass 27 t and of an endcap CsI calorimeter (16.1 X_0 thick). The electrode structure of the first layer of the cylindrical electromagnetic calorimeter, used for determining the coordinates of photons and of charged particles, is composed of alternating longitudinal and transverse strips. The energy resolution of the krypton calorimeter at an energy of 1.8 GeV comprises 3.0%, while the characteristic spatial resolution in this case reaches 1 mm. Systems for registering electrons and positrons scattered at angles within the range from 0 up to 0.01 rad with energies between 45% and 98% of the beam energy are included in the detector composition for studies of two-photon processes.

A more detailed description of the KEDR detector is given in Ref. [25].

4. Measurement of VEPP-4M collider energy

The accuracy with which the collider energy is specified and then measured is a key issue, when precision measurements are performed of the masses of elementary particles. In the course of setting the energy of the experiment, the currents of the power supplies necessary for the magnets and lenses of the accelerator are calculated by the control system. The calculation procedure is rendered complicated by most of the VEPP-4M magnets executing overlapping functions, i.e., their magnetic fields contain dipole, quadrupole, and sextopole components. A change in the current of a magnet may result in changes to the beam orbit, the betatron frequencies, and chromatism; therefore, the algorithm for calculating the current by the specified so-called setting energy is based on the results of magnetic measurements and investigation of beam behavior in the case of variation of the currents of the magnetic elements. Nevertheless, deviation of the setting energy from the true one may amount to 2–5 MeV for beam energies within the 1–5 GeV range. The reproducibility of the VEPP-4M energy in the course of hysteretic magnetization reversal cycles of the magnetic system does not exceed 0.2 MeV in the J/ψ region; in the case of a fixed setting energy, the stability of the beam energy with time remains at a level of 0.1 MeV if no significant changes occur in other collider parameters; otherwise, energy 'jumps' are observed that amount to 2 MeV. The precision values presented are clearly insufficient for studying narrow resonances, such as J/ψ and ψ(2S), or for measuring the masses of the particles produced, including ψ(3770) with a total width of about 27 MeV. To make such experiments possible, precise calibration of the beam energy by the RD method [1, 2, 26], as well as energy monitoring based on the inverse Compton scattering (ICS) method [27–29], which is less accurate but more practical and requires no preliminary beam polarization, have been realized at VEPP-4M.

4.1 Measurement of energy and of energy spread by the resonant depolarization method

The RD method, proposed at INP in 1975 [1], was applied in precise measurements of the masses of mesons: Φ [30], K^+, K^- [31], K^0 [32], ω [33], J/ψ, ψ' [34, 35], Υ, Υ', Υ'' [36–40], and of the Z-boson [41]. The relative measurement accuracy of masses in these experiments amounted to $10^{-4}-10^{-5}$ [42]. Issues of the development of the RD method and the experience of its application in experiments with the KEDR detector at the VEPP-4M collider are considered in papers [43–45].

The phenomenon of resonant depolarization is akin to that of electron and nuclear magnetic resonances. Electrons and positrons in storage rings may be spontaneously polarized owing to the action of synchrotron radiation (the Sokolov–Ternov effect) [46]; here, the polarization vector will be perpendicular to the orbital plane. The spin of an electron moving in a magnetic field undergoes precession around the magnetic field direction. In the approximation of a plane orbit, the spin precession frequency Ω only depends on the particle's Larmor revolution frequency ω and on the relativistic factor γ:

$$\Omega = \omega\left(1 + \gamma\,\frac{\mu'}{\mu}\right), \tag{1}$$

where μ'/μ is the ratio of the anomalous and normal components of the electron magnetic moment, known with an accuracy of 2.7×10^{-13} [47]. The revolution frequency ω of particles in storage rings is determined by the frequency of the accelerating voltage, and it can be set and measured with high precision. Therefore, determination of the particle energy reduces to measurement of the spin precession frequency Ω. To this end, the polarized beam is subjected to the action of an external high-frequency electromagnetic field of frequency $\Omega_{\rm dep}$, which varies slowly with time. When the condition

$$\Omega \pm \Omega_{\rm dep} = \omega n \tag{2}$$

is fulfilled with any integer n, depolarization of the beam takes place. By measuring the frequency $\Omega_{\rm dep}$ at the instant of depolarization, it is possible to determine the spin precession frequency and thus to absolutely calibrate the storage energy. The disappearance of polarization is registered by a polarimeter — a device whose readout depends on the beam polarization. For this purpose, at VEPP-4M, the dependence of the frequency of intrabunch scattering in the beam [48–50] on the degree of beam polarization is used.

The fundamental restriction imposed on the measurement accuracy of absolute energy by the RD method is significantly smaller than the energy spread in the beam. The theoretically achievable limit in accuracy, determined by the width of the frequency distribution of spin oscillations, is at a level below 1 keV. In practice, the limit of 1–2 keV on the measurement accuracy is related to distortion of the closed beam orbit, to the existence of a longitudinal magnetic field in the region of the detector, and to other factors considered in detail in Ref. [51].

In the case of work in the charmonium energy range, the characteristic time of spontaneous polarization is significantly longer than the beam lifetime in the VEPP-4M accelerator; therefore, the beam is polarized inside the VEPP-3 storage ring, after which it is injected into VEPP-4M with no significant loss of the degree of polarization.

The lifetime of such radiative polarization, which depends on the cubic mean radius of the storage ring, is very long in VEPP-4M: on the order of 100 hours at an energy of 1.8 GeV; however, the presence in the complex of the VEPP-3 booster storage ring with a significantly smaller radius permits obtaining beams with a high degree of polarization in a time of less than 1 hour. The depolarizer and polarimeter are placed in the technical section of VEPP-4M; a transverse high-frequency electromagnetic field is applied for depolarization. Particles leaving the beam as a result of intrabunch scattering are registered by a polarimeter consisting of two pairs of scintillation counters inserted in the median plane into the vacuum chamber of the storage ring. Energy calibration is performed utilizing two bunches moving in sequence: one of which is polarized, while the other one is not. The ratio $\delta \equiv f_1/f_2 - 1$, where f_1 and f_2 are the counting rates of losses of the polarized and nonpolarized bunches, respectively, undergoes a jump increase at the instant of depolarization. The counting rate of scattered particles amounts to 100–400 kHz for a beam current of 2–4 mA. In the course of energy measurement, scanning is done over the depolarizer frequency in steps of 0.06 Hz with the aid of a computer-controlled synthesizer, its linewidth proper being about 10^{-4}. The rate of frequency variation equals 0.6 Hz s^{-1}.

The characteristic jump in the relative counting rate of scattered electrons at the instant of resonant depolarization at an energy equal to the mass of $\psi(2S)$, with a degree of beam polarization superior to about 70–80%, amounts to approximately 1.5%, for a statistical confidence exceeding 10 standard deviations.

A typical dependence of the counting rate ratio ('depolarization jump') is plotted in Fig. 3. The observed linear increase preceding the RD is due to the cross sections of intrabunch scattering (and, consequently, of the particle loss) for the polarized and nonpolarized bunches differing from each other.

The RD process is slow relative to the period of synchrotron oscillations of the particle energy, which permits determining the mean spin precession frequency and, respectively, the average particle energy $\langle E \rangle$, or more correctly, the beam energy spread ($\sim 10^{-3}$). Averaging is performed both over the beam particles and over the revolution time.

The initial registration scheme of Tuschek electron pairs, usually applied in such experiments, required the coincidence of signals from scintillation counter pairs. In 2004, the direct counting mode was realized, for which such coincidences were not required, thus significantly increasing the registration

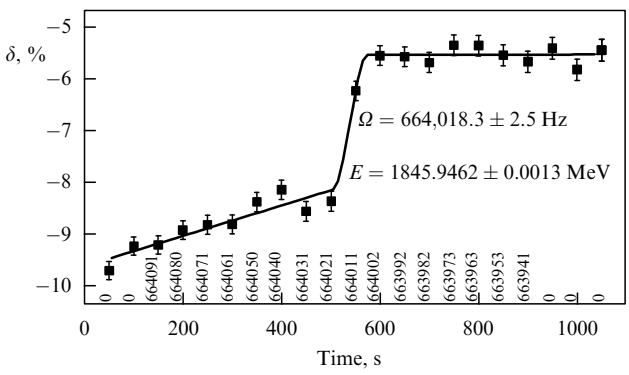

Figure 3. Ratio δ of the counting rates for the polarized and nonpolarized bunches in the case of calibration with the aid of the RD method (2002).

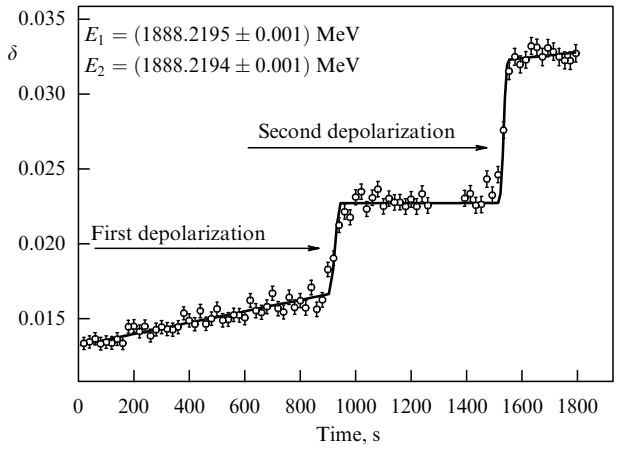

Figure 4. Partial depolarization permits carrying out twofold energy measurements with the same beams. The first measurement is performed by scanning downward in energy, while the second is done by scanning upward in energy (2004).

efficiency of intrabunch scattering events. In this mode, the counting rate of Tuschek electrons increased by more than an order of magnitude over the initial value, which reduced the time required for energy calibration to an acceptable level. Moreover, in spite of an increase in the background compared to the one in the previously applied scheme, the new technique permitted performing two, and even three, energy measurements with the same beams implementing upward and downward scanning in the depolarizer frequency. To this end, the amplitude of the depolarizer was chosen so as to provide only partial beam depolarization in the course of each scanning procedure (Fig. 4). Such a technique excludes the origination of a dangerous source of energy measurement uncertainty due to possible beam depolarization at side harmonics owing to small pulsations of the magnet currents with a frequency of 50 Hz. Pulsations may result in the energy being determined with an error, which is a multiple of approximately 25 keV.

The contribution of the masses of narrow resonances to the uncertainty, which is related to the precision of onefold calibration, does not exceed 2 keV, since energy determination is based on several RD calibrations involving opposite directions in the change of depolarizer frequency.

Partial depolarization permits performing twofold measurements of energy with the very same bunches. The first measurement involves downward scanning in energy, while the second involves upward scanning.

4.2 Measurement of energy and of energy spread by the inverse Compton scattering method

An advantage of the RD method consists in its record high precision of energy determination ($\sim 10^{-6}$), while its disadvantages lie in the long and complicated procedure for obtaining polarized beams and in the necessity of interrupting data taking in order to perform energy calibration. A method based on inverse Compton scattering (ICS) has been realized for continuous energy control. This method permits, albeit with low precision (7–10%), measuring the beam energy spread, which is also important for studying narrow resonances.

The ICS method was proposed for application at the synchrotron radiation sources BESSY-I ($E = 600$ MeV) and BESSY-II[2] ($E = 1.7$ GeV) [27, 28]. In these experiments, several joint measurements of energy were performed applying the ICS and RD techniques, and they demonstrated the possibility of determining energy, using the ICS technique, with an accuracy of 4×10^{-5}. In measurements with the KEDR detector at VEPP-4M, the ICS technique was applied for the first time in measuring the beam energy and the energy spread in elementary particle physics experiments with colliding beams [43–45]. Subsequently, INP specialists installed equipment that permits implementing the ICS technique for energy calibration at the BEPC-II electron–positron collider[3] in China [52]. At present, ICS is also tapped for monitoring the beam energy at the second INP collider — VEPP-2000 [53]

The energy $\omega_{\max}$ of gamma-quanta measured at the edge of the ICS spectrum permits us to determine the electron energy in accordance with the formula

$$\varepsilon = \frac{\omega_{\max}}{2}\left(1 + \sqrt{1 + \frac{m^2}{\omega_0 \omega_{\max}}}\right). \qquad (3)$$

The device employed for measuring the beam energy by the ICS method consists of two main parts: a single-frequency industrially constructed CO_2 laser of wavelength $\lambda = 10.6$ μm and photon energy $\omega_0 = 0.117$ eV, and a photon detector made of high-purity germanium 120 ml in volume (CANBERRA Analytical Instruments), cooled to the liquid-nitrogen temperature, with an energy resolution of 0.04% at an energy of ~ 5 MeV. For energy calibration of the germanium detector, the following radioactive sources were used: ^{60}Co, ^{137}Cs, and ^{24}Na. The energies of the calibration peaks, lying within the interval from 0.6 up to 2.7 MeV, are known with an accuracy of better than 4×10^{-6}.

The 30-W laser emits photons whose energy is stable at a level of $\Delta\omega_0/\omega_0 \simeq 10^{-8}$. The laser radiation is introduced with the aid of a system of mirrors and lenses into the vacuum chamber of VEPP-4M through the entrance window made of a ZnSe crystal. At an electron beam energy of 1.5–2.0 GeV, the edge of the Compton spectrum lies in the range of 4–7 MeV. The average counting rate of Compton photons during the experiment was at the level of 10 kHz, while the rate due to the calibration isotopes amounted to 1 kHz. The characteristic spectrum of inversely scattered Compton photons and of the calibration lines from isotopes collected during energy measurement is displayed in Fig. 5. The edge of the spectrum, which provides information on the beam energy and the energy spread, is shown in Fig. 6.

The systematic error of the method applied, found by comparing the results of energy measurements with the RD technique, amounted to 60–70 keV. About 40 min is required for collecting the spectrum and achieving a statistical accuracy of 100 keV in measuring energy during normal operation of the collider.

One of the parameters affecting the observed cross section is the beam energy spread. In calculating the masses of narrow resonances, this parameter was found directly by fitting the shape of a resonance, while in other experiments the stability of the beam energy spread was controlled by applying the ICS technique. Thus, in the experiment for measuring the mass of

[2] BESSY (German) Berliner Elecktronenspeicherring-Gesellschaft für Synchrotronstrahlung — Berlin Community of the Electron Storage Ring for Synchrotron Radiation.

[3] BEPC — Beijing Electron-Positron Collider.

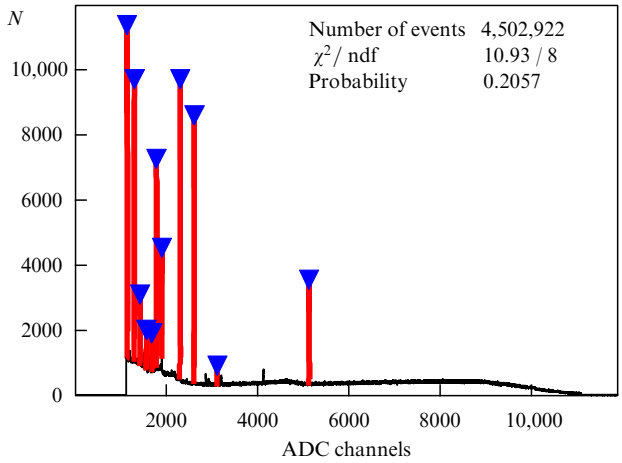

Figure 5. ICS spectrum measured at VEPP-4M. The vertical segments above the histogram correspond to the calibration isotope energies, and N is the number of events within one bin of the histogram. ADC stands for analog-to-digital converter.

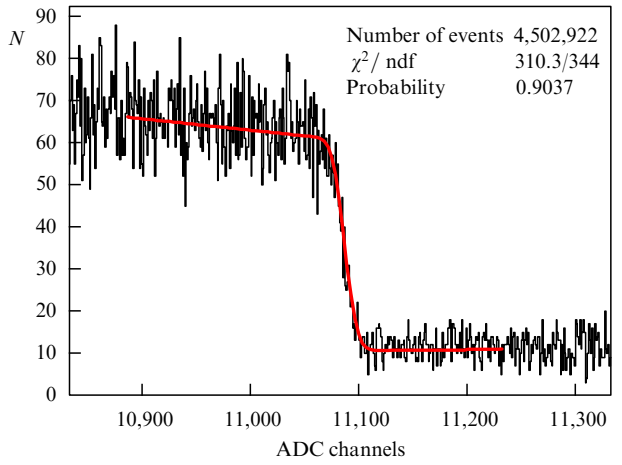

Figure 6. Edge portion of the spectrum near $\omega_{\max}$.

the τ-lepton in 2004–2006, three scans were made of the ψ(2S)-meson and one of the J/ψ-meson. The stability of the beam energy spread was controlled during the experiment with the aid of the ICS technique with an accuracy of about 7%.

5. Precise measurement of the masses of narrow resonances

We shall deal with the issue of measuring the masses of the narrow J/ψ and ψ(2S) resonances in a separate section, since, in this case, when the best possible precision has been achieved, systematic uncertainties related to the operation of the accelerator facility acquire first priority in analyzing the results of measurements.

5.1 Cross section of annihilation into hadrons in experiments devoted to measuring the masses of narrow resonances

According to Ref. [54], the one-photon annihilation cross section of an e^+e^--pair into a given final state taking into account radiative corrections can be represented as

$$\sigma(s) = \int dx \, \frac{\sigma_0\big((1-x)s\big)}{\big|1-\Pi\big((1-x)s\big)\big|^2} \, \mathcal{F}(s,x)\,, \qquad (4)$$

where the invariant s corresponds to the energy squared W of the e^+e^--pair in the center-of-mass system, $\Pi(s)$ is the total vacuum polarization operator, and $\sigma_0(s)$ is the cross section of the process in the Born approximation. The kernel of radiative corrections $\mathcal{F}(s,x)$ was calculated in Ref. [54] with an accuracy of about 0.1%, and the variable x determines a part of s lost owing to photons and soft e^+e^--pairs emitted by the initial particles.

In the soft-photon approximation, taking into account interference of the resonance process with nonresonance hadron production in the one-photon channel, expression (4) can be reduced to the form [55]

$$\sigma(W) = \frac{12\pi}{W^2}(1+\delta)\left[\frac{\Gamma_{ee}\Gamma_h}{\Gamma M}\,\mathrm{Im}\,f(W) - \frac{2\alpha\sqrt{R\,\Gamma_{ee}\Gamma_h}}{3W}\,\lambda\,\mathrm{Re}\,\frac{f^*(W)}{1-\Pi_0}\right]. \qquad (5)$$

Here, Γ, Γ_{ee}, and Γ_h are the total, electron, and hadron widths, respectively; M is the resonance mass; α is the fine-structure constant; $R = \sigma^h/\sigma^{\mu\mu}$; the parameter λ characterizes the strength of interference in the hadron cross section ($\lambda = 1$ in the case of muon pair production); in the parton model $\lambda \approx 0.38$ for J/ψ and $\lambda \approx 0.13$ for ψ(2S); function $f(W)$ is defined below, and $f^*(W)$ is the complex conjugate function of f.

Formula (5) can be traced back to Ref. [56], in which interference in the hadron cross section in the energy region of the narrow resonance was considered for the first time. The correction δ was obtained in Ref. [54] within the approach of the structure functions:

$$\delta = \frac{3}{4}\beta + \frac{\alpha}{\pi}\left(\frac{\pi^2}{3}-\frac{1}{2}\right) + \beta^2\left(\frac{37}{96}-\frac{\pi^2}{12}-\frac{1}{36}\ln\frac{W}{m_e}\right), \qquad (6)$$

$$\beta = \frac{4\alpha}{\pi}\left(\ln\frac{W}{m_e}-\frac{1}{2}\right), \qquad (7)$$

where m_e is the electron mass, and function f is defined as [57, 58]

$$f(W) = \frac{\pi\beta}{\sin\pi\beta}\left(\frac{W^2}{M^2-W^2-iM\Gamma}\right)^{1-\beta}. \qquad (8)$$

To fit the resonance, the convolution product of the cross section and the quasi-Gaussian distribution of the total collision energy is applied, which has an energy spread of σ_W in the beam:

$$G(W,W') = \frac{g(W-W')}{\sqrt{2\pi}\,\sigma_W}\exp\left[-\frac{(W-W')^2}{2\sigma_W^2}\right]. \qquad (9)$$

The pre-exponential factor $g(W-W')$, depending on the collision energy, can be written out approximately as

$$g(W-W') = \frac{1+a(W-W')+b(W-W')^2}{1+b\sigma_W^2}. \qquad (10)$$

The parameters a and b depend on the chromatism of the betatron and disperison functions at the interaction point of the beams. The second derivatives of the betatron and dispersion functions cannot be determined accurately and reliably; therefore, the coefficient b in formula (10) becomes free in the course of fitting. It is impossible to free the coefficient a owing to a subsequent drastic increase in the statistical error. The uncertainty in the measurement of mass,

caused by the difference between the pre-expontial factor and unity, is discussed in Section 5.2.

5.2 Determination of mean colliding energy of beams

The yield of resonances of mass M at the given collider energy E is determined by the probability of e^+e^--collisions with an invariant mass W close to M. Without assuming the electron and positron energies to be equal to each other, taking into account the respective radial angular and vertical dispersions, θ_x and θ_y, as well as the energy spread σ_E, we obtain upon averaging over the particle momenta [51]:

$$\langle W\rangle_p \approx \langle E_+ + E_-\rangle - \frac{1}{2}(\theta_x^2+\theta_y^2)E - \frac{\sigma_E^2}{2E} - \frac{\left(\langle E_+\rangle - \langle E_-\rangle\right)^2}{4E}\,, \tag{11}$$

where E_+ and E_- are the respective positron and electron energies. During VEPP-4M operation, in the energy region of ψ-mesons, one can assume that $W = E_+ + E_-$; the systematic uncertainty of such an approximation does not exceed 0.3 keV [51].

Since calibration of the electron energy during the experiment was performed by the RD technique and the electron and positron energies were assumed to be equal to each other in the analysis, $E_+ = E_-$, one of the essential systematic uncertainties in the measurement of the $\psi(2S)$ mass is the possible difference between the electron and positron energies.

Since the electrons and positrons travel in the same accelerator ring, the difference between their energies is determined mainly by the weak radial electric field induced in the accelerating resonators owing to the displacement of the beam orbit with respect to the axis of the resonator. Another source of difference between the electron and positron energies that has to be taken into account is the skew sextupole lense,[4] mounted at the azimuth of the vertical beam separation in the vicinity of the parasitic interaction point, so the magnetic field turns out to be distinct for electrons and positrons. Direct measurements (over 20 experiments), in which the energies of electrons and positrons were measured either simultaneously or alternatively by the RD technique [59], permitted the conclusion that the difference between the energies of the two beams does not exceed 2–3 keV.

A number of effects lead to the mean energy value W, obtained by averaging over the luminosity distribution, differing from the sum of the mean electron and positron energies. The main such effect is the existence of a small (0.8 mm) vertical dispersion function ψ_y at the interaction point, caused by electrostatic separation of the beams in the opposite section and by the inaccuracy Δ_y in convergence of the beams.

The differential luminosity can be represented as

$$\frac{\mathrm{d}L(E,W)}{\mathrm{d}W} = \frac{f_\mathrm{r}N_+N_-}{4\pi\sigma_x(W/2)\,\sigma_y(W/2)}\,\frac{1}{\sqrt{2\pi}\,\sigma_W} \times \exp\left[-\frac{1}{2}\left(\frac{W-2E}{\sigma_W} - \frac{\sigma_W\psi_y\Delta_y}{2E\sigma_y^2}\right)^2 - \frac{\Delta_y^2}{4\sigma_y^2}\right], \tag{12}$$

where f_r is the revolution frequency, N_+ and N_- are the particle numbers in the bunches, Δ_y is the beam impact parameter, and σ_x and σ_y are the effective transverse dimensions of the beam at the interaction point. As can be seen from formula (12), the vertical displacement Δ_y of the beams at the interaction point, caused by residual perturbation of the orbit related to separation of the beams, leads to the inequality $\langle W\rangle_L = \int W\,\mathrm{d}L(E,W) \neq 2E$. At the same time, inaccuracy in the aiming reduces the luminosity. Until 2006, beams were made to converge manually by the operator in such a manner that the deviation of luminosity from the maximum value was estimated to be $\sim 3\%$, which corresponds to $\Delta_y \approx 2.5$ μm for the size $\sigma_y \approx 7$ μm and results in a change in the collision energy of approximately 20 keV. The error in mass introduced by the effect considered is statistically suppressed by the large number of independent injections and in the experiments performed did not exceed 5 keV. A further reduction in this error was achieved in 2006 owing to installation of an automatic tuning system for making the beams converge on the base of the maximum luminosity.

As has already been noted, the pre-exponential factor in formula (12) depends on the collision energy owing to the chromatism of the betatron and dispersion functions at the interaction point of the beams. The logarithmic derivatives in energy of the betatron functions β_x and β_y are determined experimentally. The derivative of the ψ-function is estimated by simulation of the optical functions of the accelerator. Expansion of the pre-exponential factor leads to formula (10). Coefficient a is determined by the formula

$$a = \frac{1}{2}\frac{\beta_y'}{\beta_y} + \frac{1}{2}\frac{\beta_x'}{\beta_x}\,\frac{\sigma_{x,\beta}^2}{\sigma_{x,\beta}^2+\sigma_{x,s}^2} + \frac{\psi'}{\psi}\,\frac{\sigma_{x,s}^2}{\sigma_{x,\beta}^2+\sigma_{x,s}^2}\,. \tag{13}$$

The change in mass due to the influence of the quadratic addition determined by formula (10) does not exceed 0.5 keV, if the parameter b is free.

Such effects as a change in the energy spread, accounting for the potential of the oncoming bunch, and vertical distortion of the orbit, leading to violation of relationship (1), are dealt with in detail in Ref. [51]. The systematic uncertainty introduced by them is estimated at the level between 1 and 2 keV.

5.3 Determination of beam energy during data taking

Since the KEDR detector operated at a lower energy, the sequence of performing energy calibration and data taking in experiments with the KEDR detector differed from the respective sequence in experiments with MD-1 in the energy region of Υ-mesons, where energy calibration was performed with the 'operative beams' immediately before or after data taking. In the KEDR experiment, the energy in the course of data taking was calculated by interpolation of the results of calibrations.

The interpolation procedure for data obtained by the RD method takes into account variations in the accelerator parameters, such as the field of the turning magnets, measured by a nuclear magnetic resonance transducer, the temperature of the magnets, etc. Since variation of the energy of bunches is to a significant degree related to temperature variations of the collider perimeter, a significant role in the interpolation accuracy is played by the temperature stability of the whole accelerator. At the beginning of the experiment, in 2002, an aerial system was tapped for cooling the accelerator ring. Characteristic energy variations recorded

[4] A skew sextupole lens is a sextupole lens rotated with respect to its axis through a certain angle, which results in the appearance of additional multipole moments and which permits more precise tuning of the betatron electron and positron frequencies.

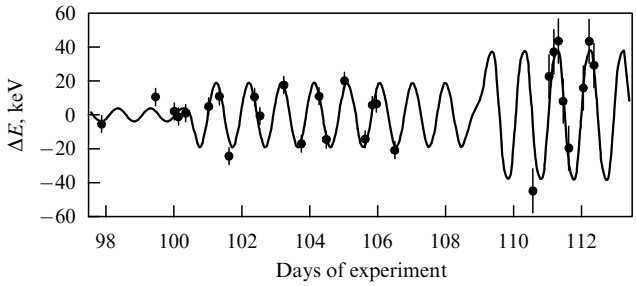

Figure 7. Variation of the VEPP-4M beam energy in time, related to diurnal fluctuations of temperature.

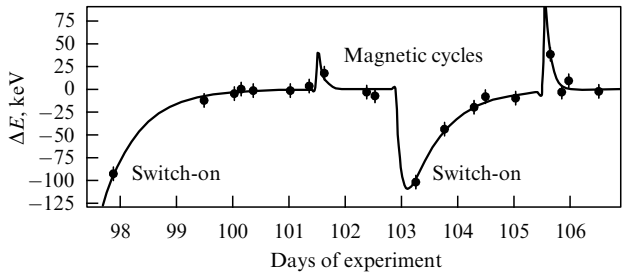

Figure 8. Variation of the VEPP-4M accelerator energy in time after switch-on and during magnetic cycles.

during data taking for a given energy setting are presented in Figs 7 and 8. Figure 7 depicts the regular variation of the accelerator energy related to diurnal temperature fluctuations. The amplitude of fluctuations increases from 4 keV in March up to 45 keV in May. Figure 8 demonstrates the irregular change in the beam energy at switch-on and during reversal magnetization of elements of the accelerator ring.

In 2004, a system operating in a thermostabilizing mode was installed for water-cooling of the collider, which permitted substantially simplifying the procedure of determining the accelerator energy.

The energy interpolation error was estimated by the difference between energies in various interpolation versions making use of different sets of parameters. The interpolation procedure and parameters describing the state of VEPP-4 are discussed in detail in Refs [51, 59]. The accuracy in determining the energy by interpolation amounts to about 7–20 keV [26], depending on the operating mode of the facility. In most of the scans of J/ψ- and ψ(2S)-mesons, the systematic interpolation uncertainty did not exceed 5 keV. An examination of several experiments performed at different times under dissimilar conditions reveals the error related to interpolation decreases.

5.4 Systematic uncertainties in cross section calculations

The uncertainties in the masses of narrow resonances due to the error in cross section calculations by formula (5) for a given value of λ do not exceed 1 keV [55]. However, as can be noted, a significant role in calculating the cross section is played by the uncertainty of the actual interference parameter λ, which specifies the strength of interference between decays of the resonance and electromagnetic nonresonant hadron productions.

Estimates of systematic uncertainties in the masses of narrow resonances, related to the value of λ, are based on variations in the value of the mass, when fits are performed considering parameter λ to be free. An alternative estimation method consists of comparing the apparent mass values in the hadron and muon channels.

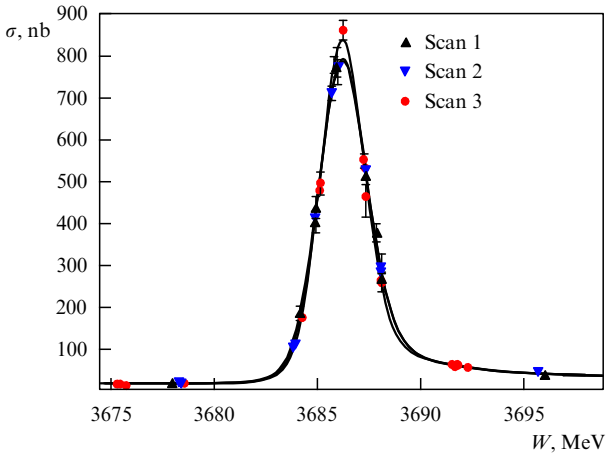

Figure 9. Hadron annihilation cross section of an electron–positron pair versus energy for three scans of ψ(2S). The experimental data are given with account of the correction for the event reconstruction efficiency obtained by simulation. The curves are the result of fitting. The difference between the results of the three scans is due to the distinction between the values of the energy spread in the scans: $\sigma_W = 1.08 \pm 0.02$, $\sigma_W = 1.06 \pm 0.01$, and $\sigma_W = 0.98 \pm 0.01$ MeV, respectively.

5.5 Results of measurements of the masses of narrow resonances

In the course of scanning, data were collected at several points on the excitation curve of the resonance. The cross section in the region of the ψ(2S)-resonance is shown in Fig. 9, where the results are presented for three scans performed in 2006.

Here, we present the mass values for the J/ψ- and ψ(2S)-mesons obtained by the KEDR Collaboration [51, 55]:

$$M_{J/\psi} = 3096.917 \pm 0.010 \pm 0.007 \text{ MeV},$$
$$M_{\psi(2S)} = 3686.114 \pm 0.007 \pm 0.011^{+0.002}_{-0.012} \text{ MeV}.$$

The indicated model-dependent uncertainty in the mass of ψ(2S), related to the assumptions of interference and dealt with in Section 5.4, was obtained in Ref. [55]. Before implementation of the KEDR experiment, the measurement accuracy in the case of narrow resonances was no better than 30 and 90 keV for the J/ψ- and ψ(2S)-mesons, respectively.

6. Measurement of the τ-lepton mass

If the mass of the τ-lepton, its lifetime, and the probability of its decay into an electron, neutrino, and antineutrino are known exactly, then a check can be made of the lepton universality principle, i.e., of one of the postulates of the Standard Model, according to which the interaction constants are all equal to each other: $g_e \equiv g_\mu \equiv g_\tau$. The relationships involving the parameters mentioned can be represented as follows:

$$\left(\frac{g_\mu}{g_e}\right)^2 = 1.028\,\frac{\Gamma(\tau \to \mu\bar{\nu}_\mu\nu_\tau)}{\Gamma(\tau \to \bar{\nu}_e\nu_\tau)}\,, \tag{14}$$

$$\left(\frac{g_\tau}{g_\mu}\right)^2 = 0.9996\,\frac{\tau_\mu}{\tau_\tau}\,\mathcal{B}(\tau \to e\bar{\nu}_e\nu_\tau)\,\frac{m_\tau^5}{m_\mu^5}\,, \tag{15}$$

where Γ and $\mathcal{B}$ are the decay probabilities.

At the time when the experiment with the KEDR detector for the precise measurement of the τ-lepton mass was being planned, the value of the τ-lepton mass was, according to data of the Particle Data Group (PDG), $M_\tau = 1776.99^{+0.29}_{-0.26}$ MeV [60]. Of the five results selected for calculation of the PDG-value of the τ-lepton mass, two — performed with the detectors DELCO (Direct ELectron COunter) and BES (BEijing Spectrometer) — were based on scans of the production threshold region of $\tau\bar{\tau}$-pairs, while the other three were based on application of the pseudomass method, first applied in the Argus experiment [61]. In spite of the quite large number of measurements, the PDG-value of the τ-lepton mass practically depended on a single measurement made in 1992 with the BES detector ($M_\tau = 1776.9^{+0.18\ +0.25}_{-0.21\ -0.17}$ MeV) [62], since the other measurements were significantly inferior to it in accuracy. Here, analysis of the published data from the BES detector revealed that the announced measurement error in the τ-lepton mass could be lowered by a factor of 1.5–2.0 [63].

Independent measurements of the τ-lepton mass, carried out by the KEDR, Belle, and BaBar collaborations over the past ten years have completely resolved the aforementioned acute issues. In this article, we shall deal with peculiarities of the KEDR experiment, which seem to be interesting from the point of view of the new experiment on measuring the τ-lepton mass, started in 2012 by the BES-III Collaboration [64].

6.1 Cross section of $e^+e^- \to \tau^+\tau^-$ process

The cross section of the $e^+e^- \to \tau^+\tau^-$ process at energy W in the center-of-mass system can be written out in the form

$$\sigma_{\rm th}(W) = \frac{1}{\sqrt{2\pi}\,\sigma_W}\int {\rm d}W'\,\exp\left[-\frac{(W-W')^2}{2\sigma_W^2}\right] \times \int {\rm d}x\,F(x,W')\,\sigma(W'\sqrt{1-x})\,. \qquad (16)$$

Here, the first integral takes the energy spread σ_W in the center-of-mass system into account, and the second one accounts for energy losses due to emission in the initial state [54], where

$$\sigma(W) = \frac{4\pi\alpha^2}{3W^2}\,\frac{\beta(3-\beta^2)}{2}\,\frac{F(\beta)F_{\rm fsr}(\beta)}{\left|1-\Pi(W)\right|^2}\,. \qquad (17)$$

The quantity $\sigma(W)$ includes the correction due to Coulomb interaction, which has the form

$$F(\beta) = \frac{\pi\alpha/\beta}{1-\exp\left(-\pi\alpha/\beta\right)}\,, \qquad (18)$$

as well as the correction due to emission in the final state, $F_{\rm fsr}(\beta)$ [65] and the effect of vacuum polarization $|1-\Pi(W)|^2$. The quantity

$$\beta = \sqrt{1-\left(\frac{2M_\tau}{W}\right)^2} \qquad (19)$$

is equal to the velocity of the τ-lepton. Owing to the Coulomb interaction of τ-leptons in the final state, the cross section of the $e^+e^- \to \tau^+\tau^-$ process (17) exhibits a step at $W = 2M_\tau$ (Fig. 10).

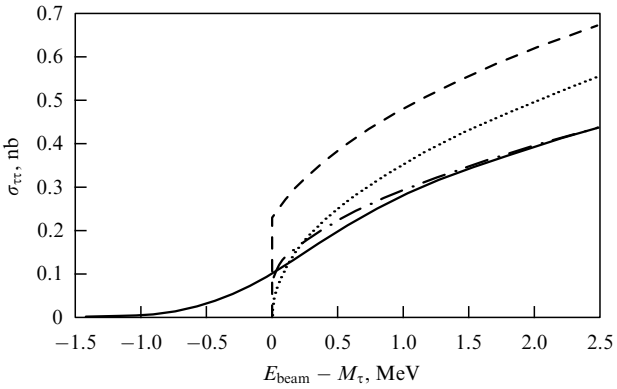

Figure 10. Cross section $\sigma_{\tau\tau}$ of the $e^+e^- \to \tau^+\tau^-$ process near the threshold versus energy. The dotted curve represents the Born approximation, the dashed curve is obtained with account of corrections for Coulomb interaction, emission in the final state, and vacuum polarization, the dot-and-dash curve takes into account corrections in the initial state, and the solid curve accounts for the energy spread in the beams.

6.2 Formulation of experimental conditions required for measurement of the τ-lepton mass

Unlike the systematic error in measurements of the masses of narrow resonances, which to a significant degree is related to the measurement accuracy of the accelerator energy, the systematic error in experiments aimed at measurement of the τ-lepton mass is mainly due to the inaccuracy in determining the registration efficiency and in measuring the luminosity and the contribution from background events. To reduce the systematic error in the indentification of $e^+e^- \to \tau^+\tau^-$ events, the softest possible selection rules were adopted in the KEDR experiment, although the background was required to be negligibly small. In this case, the following function can be used for fitting the cross section $\sigma_{\rm th}$ in the threshold region of the τ-lepton production:

$$\sigma_{\rm fit}(W) = \sigma_{\rm bg} + \varepsilon\sigma_{\rm th}(W, M_\tau)\,, \qquad (20)$$

where ε is the registration efficiency of τ-lepton decay events, and $\sigma_{\rm bg}$ is the cross section of background processes.

To ensure fulfilment of the aforementioned requirements, two-prong events were selected of the processes

$$e^+e^- \to (\tau \to e\nu_\tau\bar{\nu}_e)\,(\tau \to \mu\nu_\tau\bar{\nu}_\mu, \pi\nu_\tau, {\rm K}\nu_\tau) + {\rm c.c.},$$

where c.c. denotes the charge conjugate decay channels. As is shown in Ref. [66], when the indicated selection rules are imposed, the remaining background, which is mainly due to two-photon events, depends weakly on energy.

At the τ-lepton production threshold, the derivative in energy of the cross section has a maximum and, as a consequence, the statistics collected in this region determines the measurement error of the τ-lepton mass. The following scenario of data taking was chosen in the course of planning the experiment: 70% of the integral luminosity $\mathcal{L}$ was to be collected at three energy points: $E_{\rm beam} = M_\tau - 0.5$ MeV, M_τ, and $M_\tau + 0.5$ MeV. Here, M_τ was chosen equal to the PDG-value of the τ-lepton mass. The choice of the interval equal to 0.5 MeV between the threshold points with a high probability led to the mass being measured to be found within this range, given the uncertainty in the τ-lepton mass existing at the time. In order to measure the background level $\sigma_{\rm bg}$, 15% of the integral luminosity was collected below the τ-lepton produc-

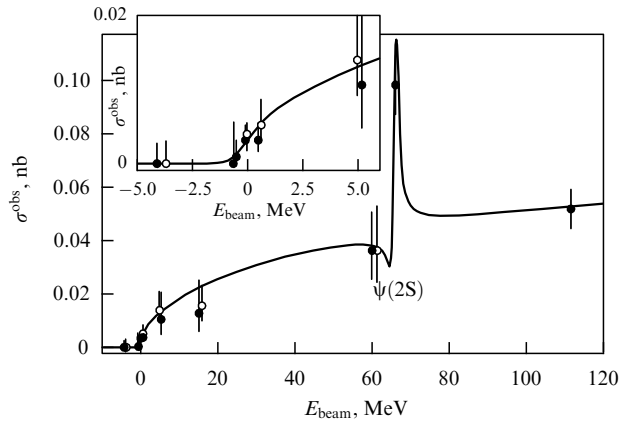

Figure 11. Observed cross section σ^{obs} of process $e^+e^- \to \tau^+\tau^-$ versus beam energy E_{beam}.

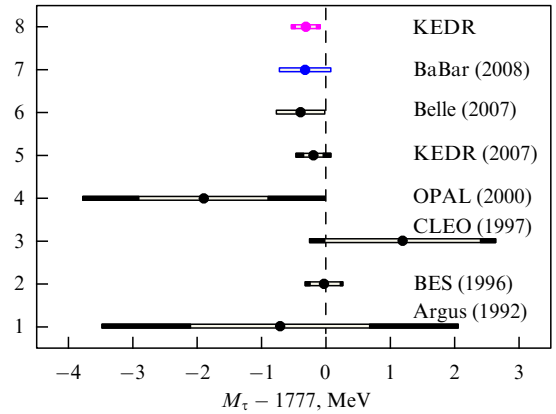

Figure 12. Values of τ-lepton mass included in the table of particle properties [47] [OPAL — Omni-Purpose Apparatus at LEP (Large Electron–Positron collider)].

tion level, and the remaining 15% was collected above this threshold with the aim of measuring the registration efficiency ε. The statistics collected above the production threshold was distributed over several points in order to enhance the fitting stability.

The experiment on measuring the τ-lepton mass consisted of two scans of the threshold region involving collection of the luminosity integral up to 15.2 pb^{-1} at nine beam energy points within the range of 1772–1889 MeV. The luminosity integral collected in the first scan amounted to 6.7 pb^{-1}, and in the second to 8.5 pb^{-1}. The distribution of the luminosity integral over the points in each scan approximately corresponded to the previously described scheme. The dependence of the measured $e^+e^- \to \tau^+\tau^-$ cross section upon energy is shown in Fig. 11.

To obtain the τ-lepton mass, the measured number of events, $N_{\tau^+\tau^-}$, at 9 beam energy points in the first scan and at 11 points in the second were fitted applying the maximum likelihood method. An independent fit of the statistics collected in both scans of the threshold region revealed that the registration efficiencies in these scans differ from each other; therefore, to obtain the τ-lepton mass on the basis of the total statistic, an additional parameter corresponding to the registration efficiency in the second scan was introduced into the fitting procedure. A joint fit of the statistics of both scans yielded the value of the τ-lepton mass:

$$M_\tau = 1776.69^{+0.17}_{-0.19}\ \text{MeV}.$$

6.3 Results of measurements of the τ-lepton mass

Systematic errors in measurements of the τ-lepton mass, due to different sources, are presented in Table 2. In the experiment with the KEDR detector, the τ-lepton mass was measured with the best accuracy in the world. The following value was obtained for the mass:

$$M_\tau = 1776.69^{+0.17}_{-0.19} \pm 0.15\ \text{MeV}.$$

As can be seen from Table 2, the main contributions to the systematic error in the mass are associated with determining the registration efficiency and with measuring the luminosity. There are reasons to imply that improvement of the analysis procedure and reprocessing of the experimental data from the KEDR detector will permit us to significantly reduce the indicated systematic uncertainties.

Table 2. Systematic errors in measurements of the τ-lepton mass.

Source of systematic error	δM_τ, keV
Stability of registration efficiency	120
Stability of luminosity measurement	80
Measurement of beam energy	35
Calculation of cross section [radiative corrections, account for interference of ψ(2S)]	30
Measurement of energy spread	20
Energy dependence of background	20
Instability of energy spread	10
Total error	150

A comparison of the results of different experiments, made use of by the PDG group, may be drawn in Fig. 12.

At present, the main contributions to the tabular value of the τ-lepton mass [47], namely

$$M_\tau = 1776.82 \pm 0.16\ \text{MeV},$$

are due to two threshold experiments performed with the BES and KEDR detectors, and two measurements made with a somewhat lower accuracy using the Belle and BaBar detectors and obtained by the method of pseudomasses. All the results are in good agreement with each other.

For enhancement of the accuracy of μ−τ-universality tests in future experiments, it is first necessary to improve the measurement accuracy of the τ-lepton lifetime and of the $\mathcal{B}_{\tau\to e\nu_\tau\bar{\nu}_e}$ decay probability, the uncertainties of which at present make the main contribution to the calculation accuracy of relationship (15). It should be noted that hopes for essential enhancement of the τ-lepton lifetime measurement accuracy in the Belle and BaBar experiments were not justified. It is possible that certain progress may be expected in ATLAS (A Toroidal LHC ApparatuS) and CMS (Compact Muon Solenoid) experiments at the Large Hadron Collider (LHC).

7. Measurement of D-meson masses

The measurement of the D-meson masses, carried out by the team of the KEDR experiment in 2005, was based on an analysis of events of the $\psi(3770) \to D\bar{D}$ process. Measurements of the mass of D-mesons, like those of the τ-lepton mass, are performed in the vicinity of the production thresh-

old, but the experimental technique used is absolutely different. In the analysis, it is the invariant mass of registered particles that is reconstructed, instead of the shape of the cross section. Owing to accurate measurement of energy by the RD method, the uncertainty in the beam energy calibration is negligibly small, which permits analyzing the data set without particle identification.

7.1 Method applied in measurement of D-meson masses

In the KEDR experiment, the D-meson masses were measured in the $e^+e^- \to D\bar{D}$ process close to the threshold by exclusive reconstruction of one of the D-mesons. D-mesons were reconstructed in $D^0 \to K^-\pi^+$ and $D^+ \to K^-\pi^+\pi^+$ decays, as well as in charge conjugate decays.

The D invariant mass may be calculated as

$$M_{\rm bc} = \sqrt{\left(\frac{W}{2}\right)^2 - \left(\sum_i \mathbf{p}_i\right)^2} \qquad (21)$$

(the so-called beam-constrained mass), where W is the total energy of the electron and positron in the center-of-mass system, and $\mathbf{p}_i$ are the momenta of the D-meson decay products. Here, advantage is taken of $\psi(3770)$ decaying into two D-mesons of the same mass and, consequently, of the same energy $W/2$ (with an accuracy up to radiative corrections). Such a change permits significantly improving the accuracy of the D-meson mass reconstruction over that of the energy calculation from the momenta of decay products. The measurement accuracy of $M_{\rm D}$ in one event is expressed in the form

$$\sigma^2_{M_{\rm D}} \simeq \frac{\sigma^2_W}{4} + \left(\frac{p_{\rm D}}{M_{\rm D}}\right)^2 \sigma^2_p = \frac{\sigma^2_W}{4} + 0.02\sigma^2_p\,. \qquad (22)$$

The contribution from the momentum resolution to the mass measurement accuracy is essentially suppressed owing to the D-meson momentum being small compared to its mass. In the vicinity of the maximum of the $\psi(3770)$ resonance, the momentum of D-mesons produced in the $\psi(3770) \to D\bar{D}$ decay amounts to $p_{\rm D} \simeq 260$ MeV.

For the reconstruction of D-mesons, it is necessary to identify events with $M_{\rm bc}$ in the region of the D mass. An additional variable also exists, with the aid of which D-decay events are conveniently identified, namely, the difference between the D-meson energy and the beam energy:

$$\Delta E = \sum_i \sqrt{m_i^2 + p_i^2} - E_{\rm beam}\,. \qquad (23)$$

In the case of D-meson decay events, the condition $\Delta E \approx 0$ must be fulfilled. In the actual analysis, events are selected from quite a broad range of the variables $M_{\rm bc}$ and ΔE near $M_{\rm bc} \sim M_{\rm D}$ and $\Delta E \sim 0$, and then the event density is fitted in these variables with account of the background; one of the fitting parameters is the D-meson mass.

7.2 KEDR experiment on measuring D-meson masses

Data taking in the KEDR experiment devoted to measuring the D-meson mass was carried out in the vicinity of the $\psi(3770)$ resonance maximum; in the course of the experiment, a luminosity integral of 0.9 $\rm pb^{-1}$ was collected.

The $e^+e^- \to D\bar{D}$ cross section in the region indicated was measured by the CLEO [67] Collaboration to be $6.57 \pm 0.04 \pm 0.10$ nb for $E = 3774$ MeV. The cross section of neutral D-meson pair production is $\sigma(D^0\bar{D}^0) = 3.66 \pm 0.03 \pm 0.06$ nb, and for a pair of charged D-mesons the cross section $\sigma(D^+D^-) = 2.91 \pm 0.03 \pm 0.05$ nb. About 100 of the sought-after events were reconstructed in the neutral mode, and 110 events in the charged one.

Table 3. Systematic errors in the measurement of D^0- and $D^\pm$-meson masses.

	δM_{D^0}, MeV	$\delta M_{D^\pm}$, MeV
Absolute momentum calibration	0.04	0.04
Description of energy loss in matter	0.01	0.03
Momentum resolution	0.13	0.10
Accounting for radiation in the initial state	0.16	0.11
Shape of signal distribution	0.07	0.05
Shape of background continuum distribution	0.04	0.09
Shape of $\delta M_{D^\pm}$-background distribution	0.03	0.06
Calibration of beam energy	0.01	0.01
Total error	0.23	0.20

The accuracy of momentum reconstruction contributes directly to the D mass measurement accuracy. Absolute calibration of the momentum scale was performed for the same set of events that was tapped in the analysis, by requiring that the mean value of ΔE be zero. As a check, alternative methods of momentum calibration were used that were based on reconstruction of the decays $K^0_S \to \pi^+\pi^-$ and $e^+e^- \to \psi(2S) \to J/\psi\pi^+\pi^-$.

The systematic uncertainties in the measurement of the D^0- and $D^\pm$-meson masses are presented in Table 3. The following values were obtained for the D-meson masses:

$$\begin{aligned} M_{D^0} &= 1865.30 \pm 0.33 \pm 0.23 \text{ MeV}, \\ M_{D^+} &= 1869.53 \pm 0.49 \pm 0.20 \text{ MeV}. \end{aligned} \qquad (24)$$

In 2007, the CLEO Collaboration measured the D^0 mass in the $D^0 \to \phi K^0_S$ decay [68]:

$$M(D^0) = 1864.847 \pm 0.150 \pm 0.095 \text{ MeV}. \qquad (25)$$

At present, the CLEO measurement determines the accuracy of the mean world value of the D^0 mass [47]; moreover, the charged D-meson mass determined via the D^0 mass and the mass difference $M_{D^+} - M_{D^0}$ is significantly more accurate than in the case of its direct determination.

The other measurements of the D-meson masses made use of in PDG calculations are significantly less accurate. They were performed in the Mark-II experiment at the e^+e^--collider SPEAR (Stanford Postitron-Electron Asymmetric Rings) [69] and by the ACCMOR (Amsterdam-CERN-Cracow-Munich-Oxford-Rutherford) Collaboration in a fixed-target experiment [70]. In both experiments, the dominant systematic error is related to the accuracy of beam energy calibration, particularly in the Mark-II measurement.

At present, our result for the charged D-meson mass is the most precise measurement value. The collected experimental statistics did not permit the KEDR experiment to compete with CLEO as far as D^0 mass measurement accuracy is concerned, but the value of the D^0 mass obtained in the KEDR experiment is important for an additional test, since the measurement was performed by a method differing from the one applied by CLEO.

8. Measurement of the ψ(3770) mass

The KEDR Collaboration's measurement of the parameters of the ψ(3770) resonance is interesting, first of all, owing to the demonstration and analysis of problems related both to the interpretation of data that are involved in the analysis of experimentally measured cross sections in the region of charmonium states and to theoretical substantiation of the applicability of the Breit–Wigner amplitude for broad resonances.

In most experimental investigations of the ψ(3770) parameters, the interference between the resonance and nonresonance amplitudes of the DD̄-pair production process has been ignored; moreover, it is chiefly the simplest form factor in the process of nonresonant DD̄-pair production that has been considered, which has led to a systematic shift of the measured resonance mass. Some of the mentioned issues were investigated within the analysis of data from the experiment dealt with in the present article.

8.1 Experiment on measuring the ψ(3770) parameters

Three joint scans in the energy region of the ψ(2S)- and ψ(3770)-resonances were performed in the KEDR experiment; the collected luminosity integral amounted to about 2.6 pb^{-1}. Measurement of the accelerator energy during the scans, as in the other aforementioned experiments, was implemented by applying the RD and ICS techniques.

The ψ(3770)-resonance parameters were determined by the joint fitting of three scans. The fitting procedure was described in detail in Refs [55, 71]. The results for the contribution associated with ψ(3770) decays and with nonresonant DD̄-pair production are given in Fig. 13.

Under the assumption of vector dominance, the main part of the cross section in the ψ(3770) region is determined by the sum of the contributions from vector resonances decaying into DD̄-pairs. In the analysis of KEDR data, simplification of the indicated model was tapped, in which the form factor of D-meson production is described by the sum of contributions from ψ(2S), ψ(3770) and of a constant term corresponding to the contribution of more distant resonances. The following value was found for the resonance mass:

$$M_{\psi(3770)} = 3779.2^{+1.8}_{-1.7}\ \text{MeV}.$$

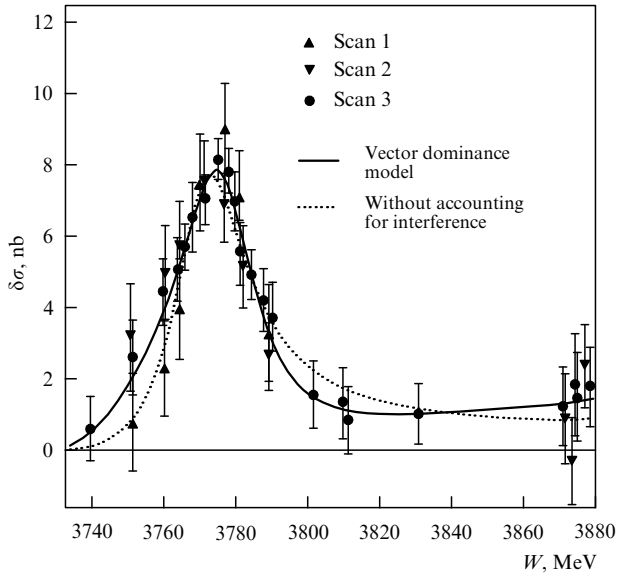

Figure 13. Contribution of $\delta\sigma$ to the $e^+e^- \to$ hadrons cross section, associated with ψ(3770) decays and nonresonant DD̄-pair production. The curves correspond to the joint fit of three scans in the vector dominance model without taking interference into account. Fitting was performed taking into account radiative corrections.

Table 4. Systematic uncertainty of the main parameters of ψ(3770) and of the nonresonance DD̄ cross section (results for two solutions are presented).

Source	$\delta M_{\psi(3770)}$, MeV
Uncertainties of a theoretical character and of 'external' parameters	
$\mathcal{B}_{n\mathrm{D\bar{D}}}$	$^{+0.0}_{-0.5}$
Characteristic interaction radius R_0 in $\Gamma(W)$	0.30
$\Gamma_{\mathrm{D^0\bar{D}^0}}/\Gamma_{\mathrm{D^+D^-}}$	0.10
D, D̄ masses	0.06
DD̄π cross section	0.15
Detector and accelerator uncertainties	
Efficiency instability	0.03
Selection criteria	0.30
Background	0.06
Luminosity measurement	0.10
Determination of energy	0.03
Total error	$^{+0.48}_{-0.69}$

The main sources of systematic uncertainty in the mass are collected in Table 4.

To estimate the model dependence of the ψ(3770) parameters, fitting was performed using alternative models for the nonresonance form factor, which were not based on the assumption of vector dominance. The resultant value of the ψ(3770)-resonance mass, obtained in the KEDR experiment, is the following:

$$M = 3779.2^{+1.8}_{-1.7}\ {}^{+0.5}_{-0.7}\ {}^{+0.3}_{-0.3}\ \text{MeV}.$$

A comparison of the results of our measurement with the results of similar experiments [72–76] reveals that ignoring interference in studies of the $e^+e^- \to$ hadrons process leads to an underestimation of the actual resonance mass. In experiments at B-factories [77–80], this tendency is less evident, and the results of ψ(3770) mass measurements happen to be within the intermediate region, which is probably explained both by the characteristic features of the analysis, being less sensitive to taking into account interference, and by measurement uncertainties.

Interference between ψ(3770) and nonresonant DD̄-pair production leads to two possible combinations of phase and lepton width in the case of a constant mass. Dealing with this interesting result — equivocation of the solution — goes beyond the scope of the present article. But it must be noted that for determination of the 'true' solution both additional theoretical studies and new experimental investigations, involving more precise determination of the probabilities of the neutral and charged modes of the $e^+e^- \to$ DD̄ process, and of possible exclusive decays of ψ(3770) into an 'other-than-DD̄ state', are required.

9. Conclusion

During the past decade, a series of experiments has been performed at the INP of the RAS SB for the precise

measurement of elementary particle masses, in which an unprecedented high-precision level was achieved. The experiments reported in the present article, which were aimed at resolving different physical problems, differ from each other both in formulation of the task and in the technique used for the analysis. At the same time, the achieved high precision of the results obtained is, to a large extent, related to the methods realized for measuring the beam energy, which permitted implementing control of the absolute accelerator energy at a new level.

It must be noted that experiments for measuring the τ-lepton and D-meson masses are good prospects for further precision enhancement in the nearest future. In experiments for the measurement of the masses of narrow resonances, no rapid significant progress is to be expected, and, most likely, the results obtained by the KEDR Collaboration in measurements of the masses of charmonium states will remain for a long time in the first rows of tabulated characteristics of elementary particles. Enhancement of the measurement accuracy of $\psi(3770)$ parameters is related to the necessity of enriching the data statistics and of developing theoretical models for the description of charmonium states above the D-meson production threshold. Only progress in both areas will permit us to determine the $\psi(3770)$ characteristics reliably.

Acknowledgments

The authors are grateful to all participants in experiments with the KEDR detector at the VEPP-4 accelerator-storage facility and note here the especially important role played in preparing and implementing the experiments discussed by V E Blinov, A V Bogomyagkov, S A Nikitin, I B Nikolaev, O A Poluektov, G M Tumaikin, and A G Shamov.

The work was carried out with a financial support from the RF Ministry of Education and Science, the Russian Foundation for Basic Research (grants 11-02-00558a, 11-02-01064a, 12-02-01076a), as well as the RF President's grant 'Support of Leading RF Scientific Schools', NSh-5320.2012.2.

References

1. Bukin A D et al., in *Vth Intern. Symp. on High Energy Physics and Elementary Particle Physics, Warsaw, 1975*, p. 138
2. Derbenev Y S et al. *Part. Accelerators* **10** 177 (1980)
3. Zholentz A A et al. *Phys. Lett. B* **96** 214 (1980)
4. Baru S E et al. *Phys. Rep.* **267** 71 (1996)
5. Anashin V V et al., in *VEPP-4M Collider*: *Status and Plans, Proc. of EPAC'98, Stockholm* (1998) p. 400
6. Aleshaev A N et al., Preprint No. 2011-20 (Novosibirsk: Budker Inst. of Nuclear Physics, Siberian Branch of Russ. Acad. of Sci., 2011)
7. Artamonov A S et al. *Phys. Lett. B* **118** 225 (1982)
8. Artamonov A S et al. *Phys. Lett. B* **137** 272 (1984)
9. Baru S E et al. *Z. Phys. C* **30** 551 (1986)
10. Baru S E et al. *Z. Phys. C* **54** 229 (1992)
11. Baru S E et al. *Z. Phys. C* **42** 505 (1989)
12. Blinov A E et al. *Phys. Lett. B* **245** 311 (1990)
13. Blinov A E et al. *Z. Phys. C* **49** 239 (1991)
14. Baru S E et al. *Z. Phys. C* **48** 581 (1990)
15. Blinov A E et al. *Yad. Fiz.* **44** 626 (1986)
16. Blinov A E et al. *Z. Phys. C* **53** 33 (1992)
17. Baru S E et al. *Z. Phys. C* **53** 219 (1992)
18. Skrinsky A N *Nucl. Instrum. Meth. Phys. Res. A* **598** 1 (2009)
19. Anashin V V et al., in *VEPP-4M Collider*: *Status and Plans, Proc. of EPAC'98, Stockholm* (1998) p. 400
20. Smaluk V V (for the VEPP-4 team), in *Accelerator Physics Issues of the VEPP-4M at Low Energy, Proc. of EPAC 2004, Luzern* (2004) p. 749
21. Blinov V E et al., in *Status of VEPP-4M Collider*: *Current Activity and Plans, Proc. of the XIX Intern. Workshop on Charged Particle Accelerators, Alushta, Crimea* (2005)
22. Alexandrov A V et al., in *Proc. of the XVIII Intern. Linear Accelerator Conf., 26–30 August 1996, Geneva, Switzerland, 15 November* (CERN 96-07) Vol. 2 (1996) p. 821
23. Anashin V V et al. *Nucl. Instrum. Meth. Phys. Res. A* **478** 420 (2002)
24. Anashin V V et al., Preprint No. 2010-40 (Novosibirsk: Budker Inst. of Nuclear Physics, Siberian Branch of Russ. Acad. of Sci., 2010)
25. Anashin V V et al. *Phys. Part. Nucl.* **44** 657 (2013) [*Fiz. Elem. Chastits At. Yadra* **44** 1264 (2013)]
26. Blinov V E et al. *Nucl. Instrum. Meth. Phys. Res. A* **494** 81 (2002)
27. Klein R et al. *Nucl. Instrum. Meth. Phys. Res. A* **384** 293 (1997)
28. Klein R et al. *Nucl. Instrum. Meth. Phys. Res. A* **486** 545 (2002)
29. Muchnoi N Yu, Nikitin S A, Zhilich V N *Conf. Proc.* **C060626** 1181 (2006)
30. Bukin A D et al. *Sov. J. Nucl. Phys.* **27** 516 (1978) [*Yad. Fiz.* **27** 976 (1978)]
31. Barkov L M et al. *Nucl. Phys. B* **148** 53 (1979)
32. Barkov L M et al. *Sov. J. Nucl. Phys.* **46** 630 (1987) [*Yad. Fiz.* **46** 1088 (1987)]
33. Barkov L M et al. *JETP Lett.* **46** 164 (1987) [*Pis'ma Zh. Eksp. Teor. Fiz.* **46** 132 (1987)]
34. Zholentz A A et al. *Yad. Fiz.* **34** 1471 (1981)
35. Zholentz A A et al. *Phys. Lett. B* **96** 214 (1980)
36. Artamonov A S et al. *Phys. Lett. B* **118** 225 (1982)
37. Artamonov A S et al. *Phys. Lett. B* **137** 272 (1984)
38. Baru S E et al. *Z. Phys. C* **30** 551 (1986); *Z. Phys. C* **32** 622 (1986)
39. MacKay W W et al. *Phys. Rev. D* **29** 2483 (1984)
40. Barber D P et al. *Phys. Lett. B* **135** 498 (1984)
41. Arnaudon L et al. (The Working Group on LEP Energy, The LEP Collaborations ALEPH, DELPHI, L3 and OPAL) *Phys. Lett. B* **307** 187 (1993)
42. Skrinskii A N, Shatunov Yu M *Sov. Phys. Usp.* **32** 548 (1989) [*Usp. Fiz. Nauk* **158** 315 (1989)]
43. Blinov V E et al. *Nucl. Instrum. Meth. Phys. Res. A* **598** 23 (2009)
44. Bogomyagkov A V et al., in *Proc. of EPAC 2006, Edinburgh, UK*
45. Blinov V E et al. *Nucl. Instrum. Meth. Phys. Res. A* **494** 81 (2002)
46. Sokolov A A, Ternov I M *Sov. Phys. Dokl.* **8** 1203 (1964) [*Dokl. Akad. Nauk SSSR* **153** 1052 (1963)]
47. Beringer J et al. (Particle Data Group) *Phys. Rev. D* **86** 010001 (2012)
48. Bernardini C et al. *Phys. Rev. Lett.* **10** 407 (1963)
49. Serednyakov S I et al. *Sov. Phys. JETP* **44** 1063 (1976) [*Zh. Eksp. Teor. Fiz.* **71** 2025 (1976)]
50. Serednyakov S I et al. *Phys. Lett. B* **66** 102 (1977)
51. Aulchenko V M et al. (KEDR Collab.) *Phys. Lett. B* **573** 63 (2003)
52. Achasov M N et al., arXiv:0804.0159
53. Berkaev D et al., in *Proc. of RUPAC 2012*
54. Kuraev E A, Fadin V S *Sov. J. Nucl. Phys.* **41** 466 (1985) [*Yad. Fiz.* **41** 733 (1985)]
55. Anashin V V et al. (KEDR Collab.) *Phys. Lett. B* **711** 280 (2012)
56. Azimov Ya I et al. *JETP Lett.* **21** 172 (1975) [*Pis'ma Zh. Eksp. Teor. Fiz.* **21** 378 (1975)]
57. Cahn R N *Phys. Rev. D* **36** 2666 (1987); *Phys. Rev. D* **40** 922 (1989)
58. Todyshev K Yu, arXiv:0902.4100
59. Nikitin S A, Thesis for Doctorate of Physics and Mathematics (Novosibirsk: Budker Inst. of Nuclear Physics, Siberian Branch of Russ. Acad. of Sci., 2007)
60. Eidelman S et al. (Partical Data Group) *Phys. Lett. B* **592** 1 (2004)
61. Albrecht H et al. (ARGUS Collab.) *Phys. Lett. B* **292** 221 (1992)
62. Bai J Z et al. (BES Collab.) *Phys. Rev. D* **53** 20 (1996)
63. Shamov A G (KEDR Collab.) *Nucl. Phys. B Proc. Suppl.* **144** 113 (2005)
64. Guangshun Huang et al. (BESIII Collab.), arXiv:1209.4813
65. Voloshin M B *Phys. Lett. B* **556** 153 (2003)

66. Anashin V V et al. (KEDR Collab.) *JETP Lett.* **85** 347 (2007) [*Pis'ma Zh. Eksp. Teor.* **85** 429 (2007)]
67. Dobbs S et al. (CLEO Collab.) *Phys. Rev. D* **76** 112001 (2007)
68. Cawlfield C et al. (CLEO Collab.) *Phys. Rev. Lett.* **98** 092002 (2007)
69. Schindler R H et al. *Phys. Rev. D* **24** 78 (1981)
70. Barlag S et al. *Z. Phys. C* **46** 563 (1990)
71. Anashin V V et al. (KEDR Collab.) *Phys. Lett. B* **711** 292 (2012)
72. Rapidis P A et al. *Phys. Rev. Lett.* **39** 526 (1977)
73. Bacino W et al. *Phys. Rev. Lett.* **40** 671 (1978)
74. Shindler R H et al. *Phys. Rev. D* **21** 2716 (1980)
75. Ablikim M et al. (BES Collab.) *Phys. Lett. B* **652** 238 (2007)
76. Ablikim M et al. (BES Collab.) *Phys. Lett. B* **660** 315 (2008)
77. Chistov R et al. (Belle Collab.) *Phys. Rev. Lett.* **93** 051803 (2004)
78. Aubert B et al. (BaBar Collab.) *Phys. Rev. D* **77** 011102(R) (2008)
79. Brodzicka J et al. (Belle Collab.) *Phys. Rev. Lett.* **100** 092001 (2008)
80. Aubert B et al. (BaBar Collab.) *Phys. Rev. D* **76** 111105(R) (2007)